



Beam section stiffness properties using 3D finite elements

Couturier, Philippe; Krenk, Steen; Høgsberg, Jan Becker

Published in:

Proceedings of the 26th Nordic Seminar on Computational Mechanics

Publication date:

2013

Document Version

Publisher's PDF, also known as Version of record

[Link back to DTU Orbit](#)

Citation (APA):

Couturier, P., Krenk, S., & Høgsberg, J. B. (2013). Beam section stiffness properties using 3D finite elements. In A. Logg, & K. A. Mardal (Eds.), *Proceedings of the 26th Nordic Seminar on Computational Mechanics* Center for Biomedical Computing, Simula Research Laboratory.

General rights

Copyright and moral rights for the publications made accessible in the public portal are retained by the authors and/or other copyright owners and it is a condition of accessing publications that users recognise and abide by the legal requirements associated with these rights.

- Users may download and print one copy of any publication from the public portal for the purpose of private study or research.
- You may not further distribute the material or use it for any profit-making activity or commercial gain
- You may freely distribute the URL identifying the publication in the public portal

If you believe that this document breaches copyright please contact us providing details, and we will remove access to the work immediately and investigate your claim.

Beam section stiffness properties using 3D finite elements

Philippe Couturier, Steen Krenk, and Jan Høgsberg

Department of Mechanical Engineering,
Technical University of Denmark, Kgs. Lyngby, Denmark
phicout@mek.dtu.dk, sk@mek.dtu.dk, jhg@mek.dtu.dk

Summary. The cross-section properties of a beam is characterized by a six by six stiffness matrix, relating the six generalized strains to the conjugate section forces. The problem is formulated as a single-layer finite element model of a slice of the beam, on which the six deformation modes are imposed via Lagrange multipliers. The Lagrange multipliers represent the constraining forces, and thus combine to form the cross-section stiffness matrix. The theory is illustrated by a simple isotropic cross-section.

Key words: cross-section analysis, coupled beam deformation, anisotropic beam

Introduction

With recent advances in manufacturing capabilities, beams with more complex geometries and materials with general anisotropy are being used in wind turbine blades. While the global response of the blades can be represented by a beam model, the accuracy depends on the use of appropriate description of the cross-section properties, including coupling from e.g. pretwist and material anisotropy. Several theories have been developed to calculate the cross-section properties of beams. Many are based on simplifications which limits their use to simple geometries or isotropic materials [1]. Two methodologies have been found to provide the correct stiffness matrix for most engineering structures which are based on advanced kinematic analysis of beams namely the theories developed by Giavotto et al. [2] and Hodges and Yu [3], respectively.

This papers presents a method to calculate the cross-section stiffness matrix of the deformation modes of classic beam theory. The method is based on the analysis of a thin slice of the beam, on which the six modes of deformation corresponding to the equilibrium modes are imposed by use of Lagrange multipliers. Each deformation mode corresponds to activating one kinematic degree-of-freedom, while setting the remaining five to zero. Thus, each kinematic load case generates six Lagrange multipliers, representing the section forces needed to impose that particular kinematic mode. Together the six sets of Lagrange multipliers, each with six components, form the cross-section stiffness matrix. The analysis is carried out by a three-dimensional finite element model of a thin slice of the beam. This format enables correct representation of effects like transverse contraction and coupling due to anisotropy.

The slice approach

The properties of a cross-section of a beam can be assessed by considering a thin slice of the beam as shown in Fig. 1. The slice is given a unit thickness for numerical simplification. The slice is characterised by six equilibrium states, namely extension, two homogeneous shear components, torsion, and two homogeneous bending components. The stiffness matrix linking the equilibrium states and their conjugate six deformation modes can be determined by imposing a displacement of the end cross-section planes of the slice and calculating the required forces. The degrees of

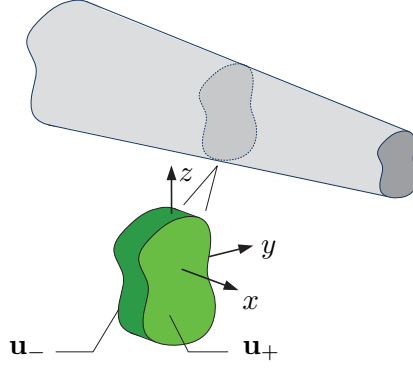


Figure 1. Unit slice of a beam with front and back face

freedom of the slice are defined in terms of the displacements at the front (+) and back (-) face of the slice as $\mathbf{u}_{\pm} = [\mathbf{u}_1^T, \mathbf{u}_2^T, \dots, \mathbf{u}_n^T]_{\pm}^T$, where n is the number of nodes and \mathbf{u}_i defines the 3D displacements at the node i .

The six deformation load cases

The properties of the slice are analysed using the finite element method. Within linear elasticity the stiffness equations of the slice take the following block matrix format

$$\begin{bmatrix} \mathbf{K}_{++} & \mathbf{K}_{+-} \\ \mathbf{K}_{-+} & \mathbf{K}_{--} \end{bmatrix} \begin{bmatrix} \mathbf{u}_+ \\ \mathbf{u}_- \end{bmatrix} = \begin{bmatrix} \mathbf{f}_+ \\ \mathbf{f}_- \end{bmatrix}, \quad (1)$$

The deformation modes are defined in terms of differences in displacement at the two sides of the slice and it is therefore convenient to rewrite the stiffness equations in terms of increments and mean values

$$\Delta \mathbf{u} = \mathbf{u}_+ - \mathbf{u}_-, \quad 2\bar{\mathbf{u}} = \mathbf{u}_+ + \mathbf{u}_-. \quad (2)$$

Substitution into (1) gives

$$\begin{bmatrix} (\mathbf{K}_{++} - \mathbf{K}_{+-} - \mathbf{K}_{-+} + \mathbf{K}_{--}) & (\mathbf{K}_{++} + \mathbf{K}_{+-} - \mathbf{K}_{-+} - \mathbf{K}_{--}) \\ (\mathbf{K}_{++} - \mathbf{K}_{+-} + \mathbf{K}_{-+} - \mathbf{K}_{--}) & (\mathbf{K}_{++} + \mathbf{K}_{+-} + \mathbf{K}_{-+} + \mathbf{K}_{--}) \end{bmatrix} \begin{bmatrix} \Delta \mathbf{u} \\ 2\bar{\mathbf{u}} \end{bmatrix} = 2 \begin{bmatrix} \mathbf{f}_+ - \mathbf{f}_- \\ \mathbf{f}_+ + \mathbf{f}_- \end{bmatrix}. \quad (3)$$

In order to define the deformation of the slice explicitly in terms of the deformation modes, the displacement vector is further transformed as to include the six generalized strains $\boldsymbol{\gamma} = [\varepsilon_x \ \varepsilon_y \ \varepsilon_z \ \kappa_x \ \kappa_y \ \kappa_z]^T$. The components ε_x , ε_y and ε_z represent the axial strain and both generalized shear strains respectively. Similarly, the components κ_x , κ_y and κ_z represent the rate of twist and both bending curvatures respectively. If one uses elements with Hermitian interpolation of the transverse displacements in the axial direction and nodal degrees of freedom defined as $\mathbf{u}_i = [u, v, w, u', v']_i^T$, the transformation is done by defining the difference in displacement, $\Delta \mathbf{u}$, as

$$\Delta \mathbf{u} = \boldsymbol{\Phi} \mathbf{u}_{\boldsymbol{\gamma}}, \quad (4)$$

where $\mathbf{u}_{\boldsymbol{\gamma}} = [\boldsymbol{\gamma}^T, \Delta u'_1, \Delta v'_1, \dots, \Delta u'_n, \Delta v'_n]^T$. The transformation matrix $\boldsymbol{\Phi}$ takes the form

$$\boldsymbol{\Phi} = \begin{bmatrix} \boldsymbol{\Gamma}_1 & \boldsymbol{\Theta}_1 & \dots & \\ \vdots & & \ddots & \\ \boldsymbol{\Gamma}_n & & & \boldsymbol{\Theta}_n \end{bmatrix}. \quad (5)$$

The matrix $\boldsymbol{\Gamma}_i$ defining the displacement increments and the matrix $\boldsymbol{\Theta}_i$ storing the rotation

increments are defined as

$$\mathbf{\Gamma}_i = \begin{bmatrix} 1 & 0 & 0 & 0 & z_i & -y_i \\ 0 & 1 & 0 & -z_i & 0 & 0 \\ 0 & 0 & 1 & y_i & 0 & 0 \\ 0 & 0 & 0 & 0 & 0 & 0 \\ 0 & 0 & 0 & 0 & 0 & 0 \end{bmatrix}, \quad \mathbf{\Theta}_i = \begin{bmatrix} 0 & 0 \\ 0 & 0 \\ 0 & 0 \\ 1 & 0 \\ 0 & 1 \end{bmatrix}, \quad (6)$$

where x_i , y_i , z_i are the global Cartesian coordinates of node i .

Elimination of $\Delta \mathbf{u}$ in (3) by (4) gives

$$\begin{bmatrix} \mathbf{\Phi}^T \mathbf{K}_{11} \mathbf{\Phi} & \mathbf{\Phi}^T \mathbf{K}_{12} \\ \mathbf{K}_{21} \mathbf{\Phi} & \mathbf{K}_{22} \end{bmatrix} \begin{bmatrix} \mathbf{u}_\gamma \\ 2\bar{\mathbf{u}} \end{bmatrix} = 2 \begin{bmatrix} \mathbf{\Phi}^T (\mathbf{f}_+ - \mathbf{f}_-) \\ (\mathbf{f}_+ + \mathbf{f}_-) \end{bmatrix}, \quad (7)$$

where \mathbf{K}_{ij} are the block components of the stiffness matrix in (3).

In order to impose the six deformation modes independently, the values of γ are defined via constraints in the form of

$$[\mathbf{C}_\gamma \ \mathbf{C}_f] \begin{bmatrix} \mathbf{u}_\gamma \\ 2\bar{\mathbf{u}} \end{bmatrix}_j = \mathbf{q}_j. \quad (8)$$

The vector \mathbf{q}_j is used to activate one kinematic degree-of-freedom, while setting the remaining five to zero, e.g. for the extension case $\mathbf{q}_1 = [1, 0, 0, 0, 0, 0]^T$. The constraints are added to the system of linear equations using the method of Lagrange multipliers where each constraint is enforced by solving for the associated Lagrange multiplier which acts as the force needed to impose the constraint [4]. As such, if no external forces are applied to the slice, the Lagrange multipliers associated with the generalized strains come out as the generalized forces. Incorporating the constraints and Lagrange multipliers, $\boldsymbol{\lambda}$, to be solved and setting the external forces to zero the system of equations takes the form

$$\begin{bmatrix} \mathbf{\Phi}^T \mathbf{K}_{11} \mathbf{\Phi} & \mathbf{\Phi}^T \mathbf{K}_{12} & \mathbf{C}_\gamma^T \\ \mathbf{K}_{21} \mathbf{\Phi} & \mathbf{K}_{22} & \mathbf{C}_f^T \\ \mathbf{C}_\gamma & \mathbf{C}_f & \mathbf{0} \end{bmatrix} \begin{bmatrix} \mathbf{u}_\gamma \\ 2\bar{\mathbf{u}} \\ \boldsymbol{\lambda} \end{bmatrix}_j = \begin{bmatrix} \mathbf{0} \\ \mathbf{0} \\ \mathbf{q}_j \end{bmatrix}. \quad (9)$$

Using this formulation, the cross-section stiffness matrix can be populated by imposing one displacement mode at a time and solving for the generalized section forces.

It is to be noted that in the case of both shear modes and torsion mode, additional constraints need to be added to enforce that the work is orthogonal to the work done in extension, and both bending cases. Since the internal work equals the external work done by the forces on the nodes, the orthogonality conditions can be expressed as

$$\mathbf{f}_{\pm\alpha}^T \mathbf{u}_{\pm\beta} = 0, \quad (10)$$

where the indices define the displacement modes based on the order set in γ , i.e. $\alpha = 1, 5, 6$ and $\beta = 2, 3, 4$.

Simple example

This section presents the analysis of a square cross-section using an implementation of the methodology described in the previous section. Eight-node elements are used with Hermitian shape functions in the thickness direction. The square has a width of $b = 2$ with a Young's modulus of $E = 1$ and Poisson's ratio of $\nu = 0.3$. The reference axis being at the center, only diagonal terms in the stiffness matrix are non-zero. Furthermore, the diagonal terms come out as EA , GA_y , GA_z , GJ , EI_y , and EI_z which are the extensional stiffness, shear stiffness about both in-plane axes, the torsional stiffness and bending stiffness about both in-plane axes, respectively.

Table 1. Normalized cross-section stiffness properties for a square

	Mesh size				Analytical
	1x1	4x4	9x9	19x19	
A/b^2	1.000	1.000	1.000	1.000	1.000
$A_y/b^2 = A_z/b^2$	1.000	0.8788	0.8424	0.8353	0.8333
J/b^4	0.1667	0.1479	0.1421	0.1409	0.1408
$I_y/b^4 = I_z/b^4$	0.09619	0.08416	0.08350	0.08338	0.08333

Results obtained using different mesh size and using analytical solutions for isotropic cross-sections are listed in Table 1, illustrating convergence for all parameters towards the analytical solution.

The associated 3D deformation of the six modes are represented graphically in Fig. 2. It can be seen that the cubic displacement associated with shear is captured. Furthermore in the two bending cases, the quadratic curvature in the thickness direction is modelled with the use of a single element via the Hermitian interpolation. Contraction from Poisson's ratio can also be observed.

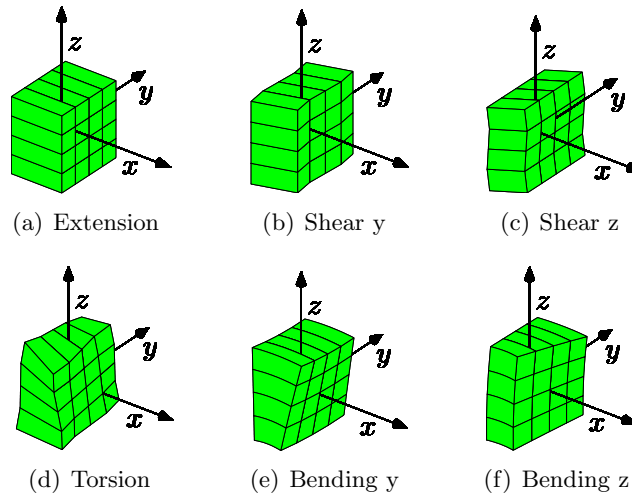


Figure 2. Elastic beam deformation modes for a square cross-section

References

- [1] H. Chen, W. Yu, and M. Capellaro. A critical assessment of computer tools for calculating composite wind turbine blade properties. *Wind Energy*, 13:497–516, 2010.
- [2] V. Giavotto, M. Borri, P. Mantegazza, G. Ghiringhelli, V. Carmaschi, G. C. Maffioli and F. Mussi. Anisotropic beam theory and applications. *Computers and Structures*, 16:403–413, 1983.
- [3] D. Hodges, W. Yu. A rigorous, engineer friendly approach for modelling realistic, composite rotor blades. *Wind Energy*, 10:179–193, 2007.
- [4] R. D. Cook et al., *Concepts and Applications of Finite Element Analysis*. Wiley, 2007.